INTERNATIONAL JOURNAL OF AUTOMOTIVE AND MECHANICAL ENGINEERING
ISSN: 2229-8649 e-ISSN: 2180-1606
VOL. 22, ISSUE 1, 2025, 12062 – 12073
DOI: https://doi.org/10.15282/ijame.22.1.2025.9.0926

RESEARCH ARTICLE

Investigation of Mechanical Properties of Groundnut-Based Composite Using the Entropy-Weighted TOPSIS Approach

Sachin G. Ghalme[1], Ibrahim Momohjimoh[2], Yogeshkumar Falak[1], Raju Kumar Thakur[3]*

[1]Faculty of Mechanical Engineering, Sandip Institute of Technology and Research Centre Nashik, 4222213 Maharashtra, India
[2]Faculty of Mechanical Engineering, Applied College, University of Hafr Al Batin, 31991 Hafr Al Batin, Saudi Arabia
[3]Faculty of Automation & Robotics, Sandip Institute of Technology and Research Centre Nashik, 4222213 Maharashtra, India

ABSTRACT – This article presents an experimental study related to groundnut shell fiber-reinforced polymer composite. The powdered groundnut shell (GNS) at different concentrations (5, 10, 15, 20, 25, 30, and 35 wt%) was utilized as reinforcement with epoxy to prepare the composite. The fabricated NaOH-treated GNS fiber/epoxy polymer composite samples underwent testing in accordance with ASTM standards to evaluate mechanical properties such as impact energy, tensile, and flexural. Maximum tensile strength (15.7 N/mm^2) and impact energy (28.86 J/mm^2) were achieved on 15 wt% GNS/epoxy composites, while maximum flexural strength (40.18 N/mm^2) was achieved on 30 wt% GNS/epoxy composite. Morphological analysis of the fabricated NaOH-treated GNS fiber/epoxy polymer composites was studied by applying SEM. The TOPSIS technique integrated with entropy weight was implemented to obtain the optimal weight proportion of GNS reinforcement in a polymer matrix to maximize tensile, flexural, and impact strength simultaneously. The entropy weight technique was employed to obtain weights for response variables. The TOPSIS method suggests 30 wt% of GNS reinforcement as optimal for maximizing desired mechanical properties. The results for optimal level reinforcement obtained through confirmatory experiments were compared to evaluate the effectiveness of the TOPSIS method.

ARTICLE HISTORY
Received : 27th Aug. 2024
Revised : 23rd Dec. 2024
Accepted : 12nd Jan. 2025
Published : 26th Feb. 2025

KEYWORDS
Groundnut fiber
Composite
Flexural
Impact
TOPSIS

1. INTRODUCTION

Composites are the combination of two or more phases to create a material with better properties. One phase is called the reinforcement, while the second phase is usually called the matrix. Using natural and synthetic fibers to reinforce the matrix phase has presented itself as a significant candidate in diverse fields like automobile, food packaging, acoustic insulations, aerospace, marine, and biomedical [1-4]. Although composite materials have unique properties, the generation of plastic waste and their non-biodegradability has created major environmental concerns [5, 6]. The growing concern over environmental degradation has motivated researchers and scientists to explore renewable and environmentally friendly materials [7, 8]. There is a need for sustainable and environmentally friendly products with significant material properties from nature's available resources [9].

Bio-based polymeric composites are of main interest to the scientific community owing to their low cost, eco-friendly characteristics, high specific properties, and abundant availability [10]. Different types of natural fibers are considered for various applications. It includes core fibers (hemp, jute, and kenaf), leaf fibers (abaca and sisal), bast fibers (hemp, flax, ramie, jute, and kenaf), seed fibers (cotton, kapok, and coir), and agriculture residues such as groundnut shell, rice, and wheat husk [11-14]. Agriculture residues are wastes generated during farming and, most of the time, disposed of by burning or dumping. Utilizing agricultural waste to develop bio-based polymeric composite will add value to agriculture waste and contribute to sustainable development by minimizing environmental pollution. Groundnut (Arachis hypogeae) belongs to the Leguminosae family and is commonly grown in some parts of the world, such as China, India, and Nigeria, which are the major producers [15]. India is the second largest groundnut producer after China, contributing about 21.03% of the world's production shares [16]. Groundnut shell is one of the major agro-waste generated, which contains cellulose (40-65%), hemicelluloses (3-15%), and lignin (26-36%) [17].

The groundnut shell (GNS) is utilized as a natural reinforcement for polymer resin, as reported in some literature. The mechanical characteristics of the GNS fiber-reinforced polymer composite were assessed by Adeosun et al. [18]. They claimed that adding GNS significantly improved the composite's mechanical qualities. In another report, Usman et al. [19] evaluated the mechanical properties of GNS/propylene composites, and a significant enhancement in the mechanical performance of recycled polypropylene was achieved with GNS inclusion. The influence of groundnut shell particle loading on the mechanical properties of hybridized sisal and groundnut shell fibers reinforced epoxy composites was studied by Soni et al. [20]. In their study, the weight fraction of sisal fiber was maintained at 30 wt% while the groundnut shell powder was varied from 0 to 20 wt%. Tensile, flexural, and hardness tests were performed on composites after they were made using the hand lay-up technique. The results showed that 15 wt% groundnut shell powder provided

***CORRESPONDING AUTHOR | Raju Kumar Thakur** | ✉ rajuiitism@gmail.com

the highest flexural strength (52 MPa) and tensile strength (23 MPa) with sisal fiber. However, when combined with sisal fiber, 20 wt% groundnut shell produced the highest mechanical hardness (20 HB).

Potadar and Kadam [21] investigated the effect of GNS particle size on the mechanical properties of GNS/epoxy composites. The weight fraction of 10% NaOH treated GNS was maintained at 30 wt% while the particle size was varied from 1 mm to 2 mm. The composite with a GNS particle size of 1 mm has the highest mechanical tensile strength (17.5 MPa) and flexural strength (60 MPa). However, lower water absorption (8%) was recorded compared to the composites with GNS particles of 2 mm (13.5%). As reported by Garcia et al. [22], a tensile strength of 23.53 MPa was achieved on 2 wt% GNS in high-density polyethylene composites prepared using the extrusion molding method. Increasing wt% of GNS beyond 2 wt% decreased mechanical properties, which was attributed to weak adhesion between GNS fiber and matrix. Besides, a decrease in the tensile strength of gypsum with GNS incorporation has been reported by Sheng et al. [23]. However, the GNS significantly influences the thermal properties of GNS/gypsum composites. Hybridization of GNS and coir fibers in equal proportion in gypsum composites significantly improved the tensile strength of gypsum. GNS fiber has been utilized in the development of biodegradable polymer composites, and results revealed that GNS in different forms (treated and untreated) promotes biodegradation of the composites by pathogenic microorganisms [24].

Although efforts have been made to utilize GNS as a natural fiber in combination with other fiber reinforcements in polymer composites, there are conflicting reports regarding the optimal volume or weight fraction of GNS fiber in the polymer matrix for achieving maximum mechanical properties. To our knowledge, no one has precisely estimated the optimal weight proportion of GNS powder in a polymer matrix for maximizing mechanical properties. In this study, an attempt has been made to evaluate the applicability of GNS fiber as reinforcement in polymer composite for mechanical application. This study aims to obtain the optimal GNS fiber weight fraction of reinforcement for simultaneously improving tensile, impact, and flexural strength. The novel approach of the weighted TOPSIS method is used to get the optimized wt% of GNS reinforcement to simultaneously maximize tensile, flexural, and impact strength.

2. METHODS AND MATERIAL

The groundnut shell (GNS) was collected from nearby farmers and powdered by grinding after cleaning it with water and drying it. Epoxy LY-556 was utilized as a matrix along with Hardener HY-951, purchased from Excellence Resin, Meerut (India). The composition of this resin is based on Bisphenol-A, which makes it suitable for high-performance FRP composites. The characteristics of matrix LY-556 are shown in Table 1. After being thoroughly cleaned with distilled water, the GNS powder was left to dry for 8 hours in the sun. For 3 hours, the GNS powder was constantly mixed while being treated with a 5% NaOH solution at room temperature. After soaking in NaOH solution for 3 hours, it was repeatedly cleaned with distilled water until all NaOH was eliminated, confirmed by the pH meter (pH nearly 7). The NaOH-treated GNS powder was dried in an oven at about 800 °C for 24 hours to remove residual moisture and obtain treated GNS powder.

Table 1. Mechanical and physical characteristics of LY-556 epoxy resin

Viscosity @25°C	10000-12000 MPas
Density @25 °C	1.15-1.2 gm/cm^3
Tensile strength	73.3 MPa
Elastic Modulus	MPa

Soaking GNS in NaOH removes the natural fats and waxes from the surface. The difference in chemical structure between fiber and matrix leads to uneven stress transfer at the interface of the NFRPCs. Surface modification with chemical treatment reacts with fiber structure, altering fiber composition and improving dispersion between natural fiber and epoxy resin, improving mechanical interlocking. This will improve stress distribution, leading to enhanced mechanical properties. Figure 1 shows the SEM image and the energy dispersive spectroscopy analysis of NaOH-treated GNS powder. In the image, porosity and roughness are visible, and this is caused by the removal of fatty materials or wax from the surface of GNS powder due to NaOH treatment.

The various proportions of GNS and matrix selected as input variables are presented in Table 2. The treated GNS varied from 5 to 35 wt% in the epoxy matrix. The homogeneous mixture of resin and hardener (10:1) was prepared by mixing and stirring properly. The calculated quantity of treated GNS powder within this mixture was mixed and stirred for another 30 minutes. The fabrication method employed in producing the composites was the hand lay-up technique. The different dimensions of test specimens were prepared by pouring this mixture into the metallic mold cavity. Before pouring the mixture, the mold's inner surface was covered with a silicon-releasing agent to remove cured samples easily. The samples were then allowed to solidify for 12 hours and meticulously removed from the mold. The comprehensive view of material components and composite fabrication process is shown in Figure 2.

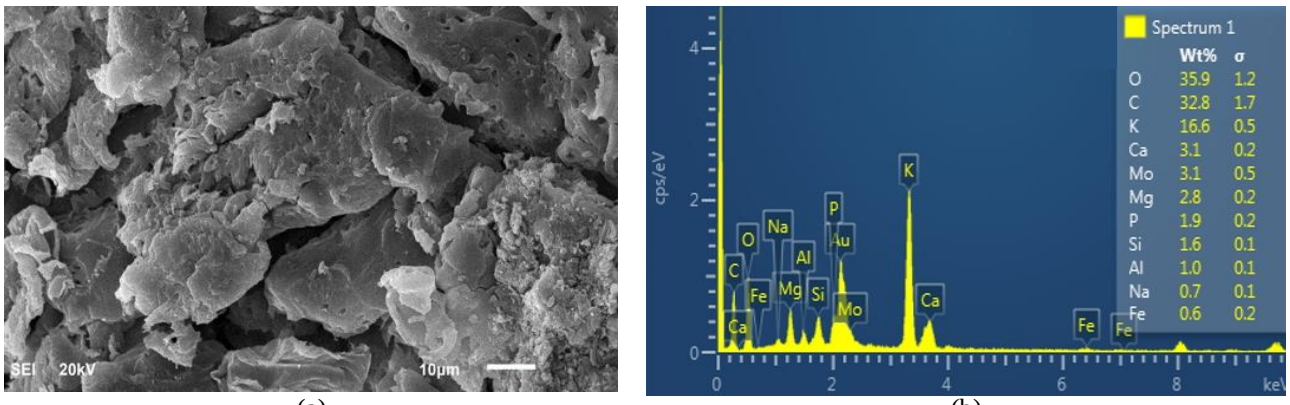

(a) (b)

Figure 1. NaOH treated GNS powder (a) SEM image, and (b) EDS outcome

Table 2. Composition of the prepared composites

GNS wt%	5	10	15	20	25	30	35
Matrix (Resin + Hardener)	95	90	85	80	75	70	65

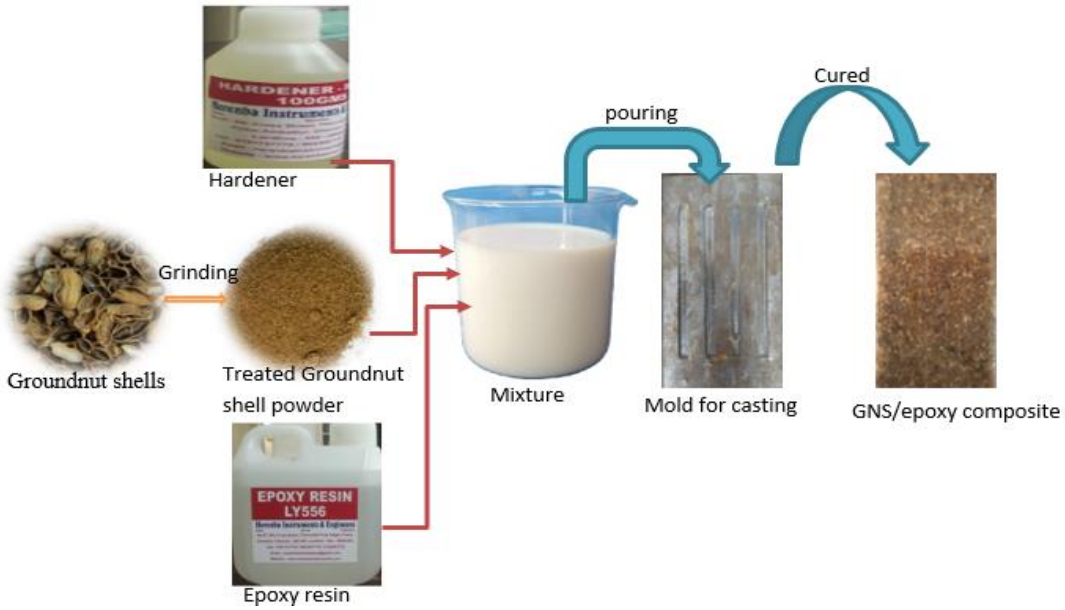

Figure 2. GNS/epoxy composite fabrication process

Every composite type was prepared in two replicates, and their water absorption characteristics were evaluated according to ASTM D570. After being dried for 24 hours at 100 °C in an oven, the specimens' dry weight was noted as W_o. The samples were submerged in distilled water at room temperature. After that, specimens were detached once every 24 hours, carefully dried with absorbent paper, weighed with an accuracy of 0.001 gm, and recorded as W_f. The average percentage of water absorption was calculated using Eq. 1.

$$\text{Water absorption \%} = \left(\frac{W_f - W_o}{W_o}\right) \times 100 \quad (1)$$

where W_f is a sample initial dry weight, W_o is a sample final wet weight.

Tensile testing allows one to understand the tensile properties of specimens and the degree to which the specimen elongates or expands till it breaks. Tensile testing was performed in compliance with ASTM D3039. The dimension of tensile test specimens was kept at 50 mm × 25 mm × 4 mm. Figure 3(a) shows the specimen along with the loading setup. The flexural test aids in the selection of materials capable of withstanding loads without bending. The material's flexural modulus can be used to determine how stiff it is. The test was carried out in compliance with ASTM D790. The dimension of flexural test specimens was kept as 65 mm × 12.5 mm × 4 mm. Figure 3(b) shows the specimen along with the loading arrangement. A Zwick/Roell DO-FB050TN universal testing machine with a load cell of 50 kN was utilized to perform tensile and flexural tests. Izod impact test was carried out using an Izod impact testing machine (Model no. EIE-PVC-07A). A swinging pendulum is used in the Izod Impact test to determine a material's resistance to impact. This test can

be used to understand the material's behavior under sudden impact loading conditions. During the test, the V-notched specimen was clamped as a cantilever beam (usually vertical). The pendulum was released to hit the specimen, and the absorbed energy was recorded on the scale. The test was performed as per ASTM D256. The dimensions of Izod test specimens were kept as 10 mm width and 4 mm thickness. The specimen used for impact testing and the test setup is shown in Figure 3(c).

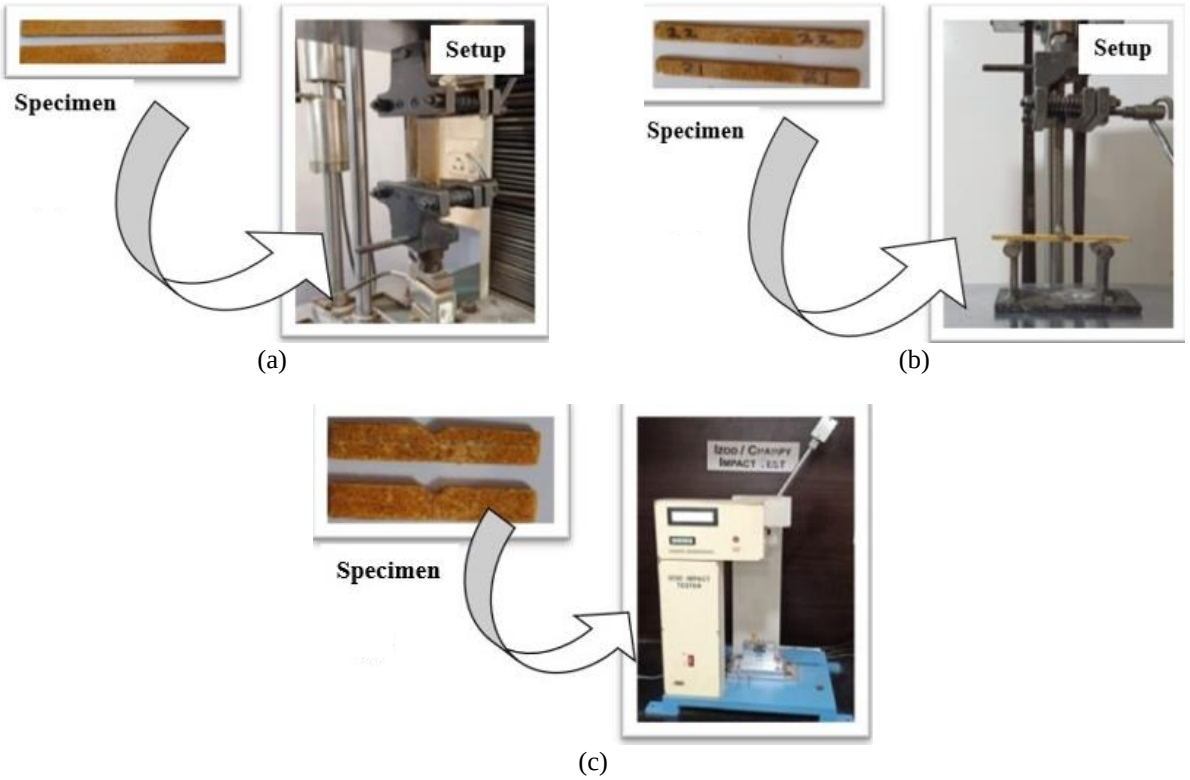

Figure 3. Test specimen and setup for (a) Tensile, (b) Flexural, and (c) Impact

3. RESULTS AND DISCUSSION

The percentage of water absorption for every sample after 10 days of duration is shown in Figure 4. The moisture absorption value for GNS fiber-reinforced epoxy polymer composite varies from 0.38% to 0.96% for 24 hrs, while that for 10 days varies from 0.96% to 4.73%. The results of the tests showed that the moisture level in the specimen increased with time, and then it became stable. The percentage of moisture absorption also increases with an increase in filler proportion in composite specimens. The cell wall polymer of the material contains oxygen-containing groups or hydroxyl that perform a substantial role in water attraction through hydrogen bonding. Increasing the weight fraction of GNS in the epoxy matrix translated to an enhancement in the number of hydrogen bonds, and this explained the rise in water absorption with GNS addition.

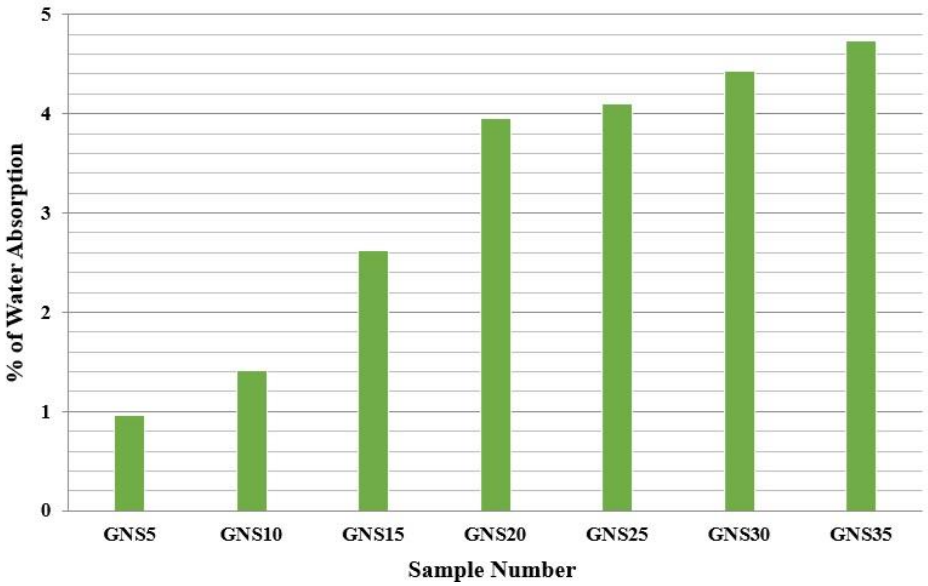

Figure 4. Water absorption of specimens for 10 days

Moreover, due to moisture, the cell wall swells and causes expansion of the specimen until the cell walls are saturated with water. So, after a specific interval, the percentage of water absorption became stable. Compared to the previous studies [25, 26], the water absorption of the fabricated GNS/epoxy composites reported in this study is much lower, possibly due to the GNS treatment at the appropriate concentration and time employed prior to its incorporation in the matrix.

The tensile test results are presented in Figure 5. The epoxy's tensile strength initially increased with GNS loading up to 15 wt%. Further loading of GNS in an epoxy matrix decreases the tensile strength of GNS/epoxy composites. It is interesting to know that the maximum tensile strength value achieved in this work is higher than the maximum tensile strength (2.6 MPa) reported in the epoxy-containing 20 wt% NaOH GNS treated fiber composite [27]. However, a slightly higher value (17.5 N/mm2) of tensile strength was reported in the reference [21], containing 30 wt % NaOH GNS treated fiber in the epoxy composite.

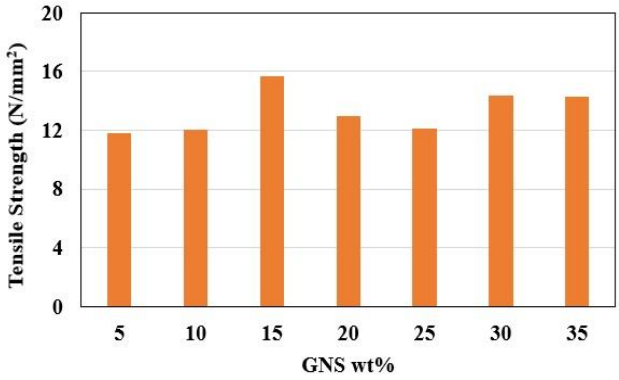

Figure 5. Tensile strength of various GNS wt% composite

The SEM fracture surface images of selected GNS/epoxy composite are shown in Figure 6. The incorporation of 5 wt% GNS in epoxy (Figure 6(a)) showed insufficient GNS to form strong bonds with the epoxy matrix as GNS is increased to 15 wt% (Figure 6(b)), the micro and macro voids were substantially filled, showing the significant increase in tensile test results. Further increases in GNS concentration beyond 30 wt% (Figure 6(c)) promoted the formation of GNS clusters or agglomerates. These GNS clusters reduced the tensile strength as they might create stress concentration points in the composite structure.

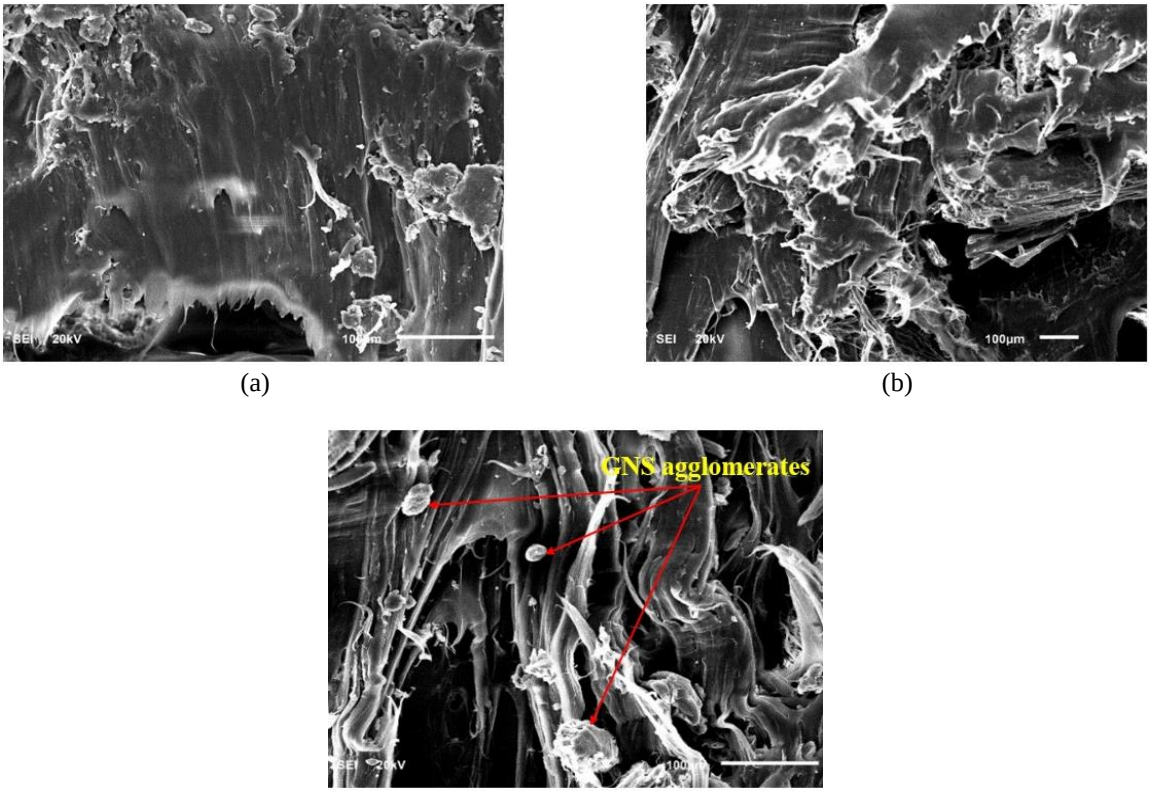

Figure 6. SEM pictures of tensile fractured zone of (a) 5 wt% GNS, (b) 15 wt% GNS, and (c) 30 wt% GNS

Flexural strength initially increased with GNS inclusion and decreased to 30 wt% GNS afterward, as shown in Figure 7. Maximum tensile strength (15.7 N/mm^2) and flexural strength (40.18 N/mm^2) were achieved at 15 wt% and 30 wt% GNS loading, respectively. For the impact strength of the GNS/epoxy polymer composites, the trend is almost like the tensile strength result, as maximum impact energy (28.86 J/mm^2) was achieved at 15 wt % GNS incorporation, as shown in Figure 8. The initial increase in tensile strength of the GNS/epoxy composites with GNS inclusion may be attributed to the filling of the voids between the epoxy matrix and the effective dispersion of the GNS within the epoxy. Further loading beyond 15 wt% GNS decreased the tensile performance of GNS/epoxy composites, and this may be due to the presence of agglomerates within the epoxy, as equally observed in the literature [28-30].

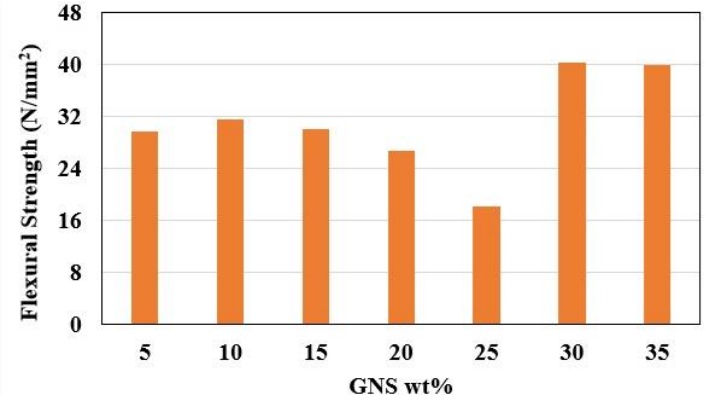

Figure 7. Flexural strength of different GNS wt% composites

The filler agglomeration of the GNS particles could generate stress concentration locations and decrease the overall strength of composites. Besides, insufficient interfacial bonding may lead to poor load transfer between fiber and epoxy, which equally contributes to strength reduction at higher fiber loading. Particle clustering also affected the trend of the result noticed in the flexural strength of GNS/epoxy composites, although this became significant beyond 30 wt% GNS. Overall, the flexural strength of epoxy/fiber polymer composites increases with enhancing particle concentration. The impact energy of GNS/epoxy composites is directly influenced by hydrogen bonds between the fibers, which are often weaker than the fibers themselves. However, the area available for bonding between the fibers varies depending on the characteristic thickness, length, and level of treatment [31].

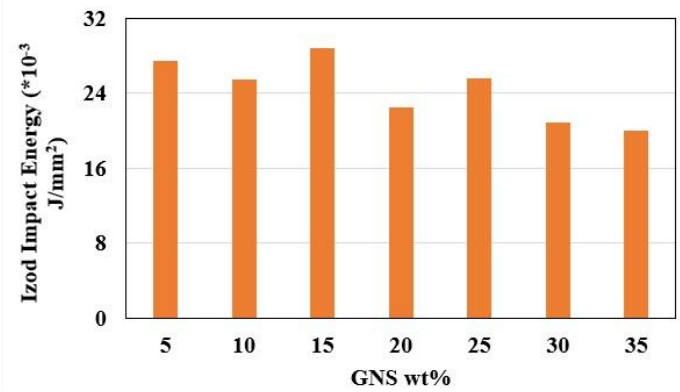

Figure 8. Impact energy of different GNS wt% composite

Shannon and Weaver proposed the Entropy Weight Method (EWM) [32], and then Zeneley enhanced it in 1982. When it comes to Multi-Criteria Decision Making (MCDM), EWM is a useful tool for allocating weights to the selected criteria or responses [33-35]. Wang et al. [31] claim that the EWM can solve the shortcomings of the subjective weighing approach since it is an objective weighing procedure founded on impartial data. One very effective method for determining weights to access response indications is the EWM. The steps for calculating EW are as follows [34]:

- Step I: Normalization of decision matrix

If n response variables have m values, the decision matrix looks like this:

$$A = \left(a_{ij}\right)_{mn} = \begin{bmatrix} a_{11} & \cdots & a_{1n} \\ \vdots & \ddots & \vdots \\ a_{m1} & \cdots & a_{mn} \end{bmatrix} \quad (2)$$

The response variables may have different units. Normalizing data inside the 0–1 range is required. The advantageous response is normalized using Eq. 3, and the non-beneficial response is normalized using Eq. 4.

$$NMa_{ij} = \frac{a_{ij}}{Maxa_{ij}} \quad (3)$$

$$NMa_{ij} = \frac{Mina_{ij}}{a_{ij}} \tag{4}$$

In this work, all three responses are mechanical properties and are desirable/beneficial; therefore, Eq. 3 is utilized for normalization.

Eq. 5 is utilized to determine the response's probability following normalization.

$$P_{ij} = \frac{a_{ij}}{\sum_{i=1}^{m} a_{ij}} \tag{5}$$

- Step II: Computation of entropy of every index

$$E_j = -\frac{1}{lnm}\sum_{i=1}^{m} P_{ij}.lnP_{ij}, \;\; j = 1,2,3 \ldots . n \tag{6}$$

- Step III: Computation of degree of deviation of every response

$$D_j = \left|1 - E_j\right|, \;\; j = 1,2, \ldots . n \tag{7}$$

where the degree of deviation of the crucial data for the j^{th} criterion is measured by D_j.

- Step IV: Computation of Entropy's weight

$$w_j = \frac{D_j}{\sum_{j=1}^{m} D_j} \tag{8}$$

where w_j is the j^{th} criteria's significant weight.

Table 3 displays the entropy weight computation and percentage weighting for each response.

Table 3. Entropy weight calculation

Calculation	Tensile strength	Flexural strength	Impact strength
$\sum_{i=1}^{m} P_{ij}.lnP_{ij}$	-1.6531	-1.6066	-1.6868
$E_j = -\frac{1}{lnm}\sum_{i=1}^{m} P_{ij}.lnP_{ij}$	0.8495	0.8257	0.8668
$D_j = \left\|1 - E_j\right\|$	0.1505	0.1744	0.1332
$w_j = \frac{D_j}{\sum_{j=1}^{m} D_j}$	0.3285	0.3807	0.2907
% Weight	32.85	38.07	29.07

TOPSIS is one of the appropriate and straightforward methods for obtaining multi-response optimization solutions in multi-criteria decision-making [35-37]. The foundation of TOPSIS is the one in which the optimal solution is closest to the positive ideal solution and furthest from the negative ideal solution. TOPSIS offers a solution that is the furthest from the worst-case scenario and the closest to the best-case scenario. In the field of optimization, several studies used TOPSIS. The following describes the TOPSIS method's step-by-step application in the ongoing research project:

- Step I: Construction of decision matrix

Eq. 9 states that in multi-objective TOPSIS situations, the averaged values of each output response for each experiment are grouped into a matrix called a decision matrix.

$$D = \begin{bmatrix} x_{11}x_{12}x_{13} \cdots \cdots x_{1n} \\ x_{21}x_{22}x_{23} \cdots \cdots x_{2n} \\ x_{31}x_{32}x_{33} \cdots \cdots x_{3n} \\ \cdots\cdots\cdots\cdots\cdots\cdots \\ \cdots\cdots\cdots\cdots\cdots\cdots \\ x_{m1}x_{m2}x_{m3} \cdots \cdots x_{mn} \end{bmatrix} \tag{9}$$

where *n* represents response variables with m corresponding alternatives/values.

- Step II: Normalization of decision matrix

The response variables could be in various scales and dimensions. Converting them into non-dimensional attributes is necessary to compare them mutually across the criteria. The decision matrix is further normalized using Eq. 10.

$$r_{ij} = \frac{x_{ij}}{\sqrt{\sum_{i=1}^{m} x_{ij}^2}}, i = 1,2, \ldots . m; j = 1,2, \ldots . n \quad (10)$$

- Step III: Computation of weighted normalized matrix

The normalized response variables are now multiplied by the appropriate weights that were determined using the previously described entropy weight computation. The outcomes of weights are 31.28% for tensile strength, 34.70% for flexural strength, and 34.015% for impact strength. Eq. 11 is utilized to determine the weighted normalized matrix.

$$v_{ij} = w_j * r_{ij}, i = 1,2, \ldots . m; j = 1,2, \ldots . , n \quad (11)$$

Table 4 displays the values of the weighted normalized matrix and normalized matrix for impact, flexural, and tensile strength.

Table 4. Values of normalized and weighted normalized response variables

Specimen number	Normalized matrix for response variables			Weighted normalized matrix for response variables		
	Tensile strength	Flexural strength	Impact strength	Tensile strength	Flexural strength	Impact strength
GNS5	0.33288	0.35443	0.42224	0.10935	0.13493	0.12274
GNS10	0.33881	0.37641	0.39188	0.11130	0.14330	0.11392
GNS15	0.44290	0.35843	0.44352	0.14549	0.13646	0.12893
GNS20	0.36673	0.31806	0.34578	0.12047	0.12108	0.10052
GNS25	0.34191	0.21568	0.39265	0.11232	0.08211	0.11414
GNS30	0.40482	0.47998	0.32158	0.13298	0.18273	0.09348
GNS35	0.40369	0.47556	0.30705	0.13261	0.18105	0.08926

- Step IV: Evaluation of positive ideal (best) and negative ideal (worst) solution

The intended response variables are increased by a positive ideal solution (best) and decreased by a negative ideal solution (worst). Equations 12 and 13 are used to compute positive ideal and negative ideal solutions, respectively.

The positive ideal solution:

$$A^+ = \{v_1^+, v_2^+, \ldots \ldots . v_n^+\} = \left\{\left(max_i v_{ij} \middle| j \epsilon J\right), \left(min_i v_{ij} \middle| j \epsilon J'\right) | 1, \ldots . m\right\} \quad (12)$$

The negative ideal solution:

$$A^- = \{v_1^-, v_2^-, \ldots \ldots . v_n^-\} = \left\{\left(min_i v_{ij} \middle| j \epsilon J'\right), \left(max_i v_{ij} \middle| j \epsilon J\right) | 1, \ldots . m\right\} \quad (13)$$

where, $J = \{j = 1,2, \ldots \ldots n | j\}$: $Associated\ with\ beneficial\ response\ variables$

$J' = \{j = 1,2, \ldots \ldots nj | j\}$: $Associated\ with\ non - beneficial\ response\ variables$

Table 5 displays the evaluated values of negative-ideal (worst) and positive-ideal (best) solutions.

Table 5. Values of positive ideal and negative ideal solution

Response variable	Positive ideal solution	Negative ideal solution
Tensile strength	0.14549	0.10935
Flexural strength	0.18273	0.08211
Impact strength	0.12274	0.08926

- Step V: Computation of distance from ideal solution

Calculate each alternative's distance from the positive ideal solution (S_i^+) and the negative ideal solution (S_i^-), using Eq. 14 and 15, respectively.

$$S_i^+ = \sqrt{\sum_{j=1}^{n} \left(v_{ij} - v_j^+\right)^2}, \quad i = 1,2, \ldots . m \quad (14)$$

$$S_i^- = \sqrt{\sum_{j=1}^{n} \left(v_{ij} - v_j^-\right)^2}, \quad i = 1,2, \ldots . m \quad (15)$$

where the distances S_i^- and S_i^+ represent the i[th] and j[th] alternative's distance from negative ideal solution and positive ideal solution, respectively.

Table 6 displays the estimated values of each alternative's separation from the negative and positive-ideal solutions.

Table 6. Values of positive and negative separation distance

Specimen no.	Positive separation distance	Negative separation distance
GNS5	0.05992	0.08259
GNS10	0.05293	0.08207
GNS15	0.04669	0.09547
GNS20	0.07014	0.05784
GNS25	0.10630	0.05496
GNS30	0.03182	0.10888
GNS35	0.03591	0.10597

- Step VI: Closeness coefficient of each alternative solution

Using Eq. 16, determine how near each alternative is to a positive ideal solution.

$$C_i = \frac{S_i^-}{S_i^+ + s_i^-} \tag{16}$$

where, $0 < C_i \leq 1, i = 1,2, \ldots \ldots m$

- Step VII: Ranking preference order

It is necessary to maintain the ranking order in descending order from 0 to 1, considering the closeness coefficient (C_i) values. Of the several response variables used in decision-making, the value that is closest to 1 has achieved the first rank and is chosen as the best alternative. Table 7 presents the evaluated values and accompanying ranking for each experiment or alternative.

Table 7. Values of closeness coefficient and ranking

Specimen no.	Closeness coefficient	ranking
GNS5	0.5795	5
GNS10	0.6079	4
GNS15	0.6716	3
GNS20	0.4519	6
GNS25	0.3408	7
GNS30	0.7738	1
GNS35	0.7469	2

It is possible to infer from the computation and closeness coefficient shown in Table 8 that the closer coefficient value with the larger value corresponds to experiment 6 with 30% wt. of GNS powder and 70% of the solution is an optimal combination in NFRPC to achieve maximum strength in tensile, flexural and impact loading conditions.

After evaluating optimal reinforcement using TOPSIS, the samples were prepared with optimal GNS powder reinforcement for the confirmatory experiment. The confirmatory test was conducted twice; the outcomes are presented in Table 8.

Table 8. Results from confirmatory experiment

Sr. no.	Wt% of GNS powder reinforcement	Avg. tensile strength (N/mm^2)	Avg. flexural strength (N/mm^2)	Avg. izod impact energy ($*10^{-3}$ J/mm^2)
1	30	14.850	40.950	21.086
2	30	14.560	40.260	21.260
Average		14.705	40.605	21.173

The results of the confirmatory experiment were compared with the minimal/initial reinforcement condition of 5% wt. of GNS powder and the condition of poor reinforcement as 15% wt of GNS powder. Table 9 displays the outcomes of the comparison. For the confirmatory experiment, the closeness coefficient was computed to be 0.7822. It is clear from Table 9 that there is a significant improvement in tensile, flexural, and impact strength with 30% wt addition of GNS

powder in the solution. The improvement in closeness coefficient for the closeness coefficient w.r.t basic reinforcement condition is about 34.97%.

Table 9. Comparison of confirmatory experiment results

	Basic reinforcement	Poor reinforcement	Optimal reinforcement	
			Predicted	Experimental
wt% of GNS Powder	5	25	30	30
Tensile strength	11.8000	12.1200	14.3500	14.7100
Flexural strength	29.6700	18.0550	40.1800	40.6100
Impact strength	27.4750	25.5500	20.9250	21.1700
Closeness coefficient	0.5795	0.3408	0.7738	0.7822
% Improvement w.r.t basic reinforcement condition				34.97%

4. CONCLUSIONS

The work's main goal was to determine and propose optimal reinforcement of groundnut shell powder in epoxy composite to maximize the flexural, tensile, and impact strength. This work also investigated the feasibility of utilizing NaOH-treated groundnut shell (GNS) powder as a reinforcing material for an epoxy polymer matrix for improved mechanical properties. Multi-objective optimization has been performed using TOPSIS to obtain the optimal reinforcement for presenting improved mechanical properties. The primary conclusions of the current study are as follows:

- The 15 wt% NaOH treated GNS powder reinforcement improves tensile and impact strength. However, the flexural strength was poor at this concentration of GNS in the epoxy matrix. The statistical analysis using entropy-weighted TOPSIS suggested 30 wt% GNS powder as the optimal reinforcement for significantly improved mechanical properties to basic reinforcement proportion.
- The 15 wt% GNS/epoxy composites had the highest tensile strength (15.7 N/mm^2) and impact energy (28.86 J/mm^2), while 30 wt% GNS/epoxy composites had the highest flexural strength (40.18 N/mm^2).
- Confirmatory experiments reveal the improvement in the closeness coefficient for the optimal and initial setting using TOPSIS, which is 34.97%.
- The optimal reinforcement suggested by the TOPSIS method is acceptable, as we could see significant improvement in tensile and flexural strength with a slight decrement in impact strength.
- The water absorption rate was low compared to other agro-waste-based composites. This improvement may be due to lower void space and proper bonding between NaOH-treated GNS powder and epoxy matrix.

CONFLICT OF INTEREST

The authors declare that there is no conflict of interest.

AUTHORS CONTRIBUTION

Sachin G. Ghalme (Writing - original draft; Conceptualization; Formal analysis; Visualisation; Supervision)

Ibrahim Momohjimoh (Data curation; Writing - original draft; Resources)

Yogeshkumar Falak (Methodology; Visualisation; Supervision)

Raju Kumar Thakur (Writing - original draft; Methodology; Visualisation; Supervision)

ACKNOWLEDGEMENT

The authors acknowledge the faculty of engineering, Sandip Foundation Group for providing the equipment.

REFERENCES

[1] R. K. Thakur, K. K. Singh, "Abrasive waterjet machining of fiber-reinforced composites: A state-of-the-art review," *Journal of Brazillian Society of Mechanical Science and Engineering*, vol. 42, pp. 381, 2020.

[2] R. K. Thakur, K. K. Singh, "Influence of fillers on polymeric composite during conventional machining processes: a review," *Journal of Brazillian Society of Mechanical Science and Engineering*, vol. 43, pp. 94, 2021.

[3] R. K. Thakur, K. K. Singh, "Evaluation of advanced machining processes performance on filler-loaded polymeric composites: a state-of-the-art review," *Journal of Brazillian Society of Mechanical Science and Engineering*, vol. 43, pp. 300, 2021.

[4] R. K. Thakur, K. K. Singh, Mahesh, P. Rawat, "Evaluation of graphene nanoplatelets addition and machining methods on the hole quality and bearing strength of glass and carbon fiber reinforced epoxy laminates." *Journal of Manufacturing Processes*, vol. 115, pp. 137-155, 2024.

[5] G. M. Kanaginahal, S. Hebbar, K. Shahapurkar, M. A. Alamir, V. Tirth, I. M. Alarifi, M. Sillanpaa, H. C. A. Murthy, "Leverage of weave pattern and composite thickness on dynamic mechanical analysis, water absorption and flammability response of bamboo fabric/epoxy composites," *Heliyon*, vol. 9, pp. e12950, 2023.

[6] B. H. H. Goh, H. C. Ong, M. Y. Cheah, W. H. Chen, K. L. Yu, T. M. I. Mahlia, "Sustainability of direct biodiesel synthesis from microalgae biomass: A critical review. Renew," *Sustainable Energy Review*, vol. 107, pp. 59-74, 2019.

[7] A. T. Oyewo, O. O. Oluwole, O. O. Ajide, T. E. Omoniyi, M. A. Hussain, "A summary of current advancements in hybrid composites based on aluminium matrix in aerospace applications," *Hybrid Advances*, vol. 5, pp. 100117, 2024.

[8] M. R. Sanjay, S. Siengchin, J. Parameswaranpillai, M. Jawaid, C. I. Pruncu, A. A. Khan, "comprehensive review of techniques for natural fibers as reinforcement in composites: Preparation, processing and characterization," *Carbohydrate Polymers*, vol. 207, pp. 108-121, 2019.

[9] M. M. Zagho, E. A. Hussein, A. A. Elzatahry, "Recent overviews in functional polymer composites for biomedical applications," *Polymers*, vol. 10, pp. 739, 2018

[10] S. H. Kamarudin, M. S. M. Basri, M. Rayung, F. Abu, S. Ahmad, M. N. Norizan, S. Osman, N. Sarifuddin, M. S. Z. M. Desa, U. H. Abdullah, I. S. M. A. Tawakkal, L. C. A. Abdullah, "A review on natural fiber reinforced polymer composites (NFRPC) for sustainable industrial applications," *Polymers*, vol. 14, pp. 1-36, 2022.

[11] K. L. Pickering, M. G. A. Efendy, T. M. Le, "A review of recent developments in natural fiber composites and their mechanical performance," *Composites Part A: Applied Science and Manufacturing*, vol. 83, pp. 98-112, 2016.

[12] O. Faruk, A. K. Bledzki, H. P. Fink, M. Sain, "Biocomposites reinforced with natural fibers: 2000-2010," *Progress in Polymer Science*, vol. 37, pp. 1552-1596, 2012.

[13] L. Kerni, S. Singh, A. Patnaik, N. Kumar, "A review on natural fiber reinforced composites," *Materials Today Proceedings*, vol. 28, pp. 1616-1621, 2020.

[14] S. Routray, A. Sundaray, D. Pati, A. K. Jagadeb, "Preparation and Assessment of Natural Fiber Composites for Marine Application," *Journal of The Institution of Engineers (India):Series D*, vol. 101, pp. 215-221, 2020.

[15] M. A. Usman, I. Momohjimoh, A. O. Usman, "Characterization of groundnut shell powder as a potential reinforcement for biocomposites," *Polymers Form Renewable Resources*, vol. 12, pp. 77-91, 2021.

[16] Usman, A. B. Taiwo, D. Haratu, M. A. Abubakar, "Socio-Economic Factors Affecting Groundnut Production in Sabongari Local Government of Kaduna State Nigeria," *International Journal of Food and Agricultural Economics*, vol. 1, pp. 41-48, 2013.

[17] N. Sathiparan, A. Anburuvel, V. V. Selvam, "Utilization of agro-waste groundnut shell and its derivatives in sustainable construction and building materials – A review," *Journal of Building Engineering*, vol. 66, pp. 105866, 2023.

[18] S. Adeosun, O. Taiwo, E. Akpan, S. Gbagba, S. Olaleye, "Mechanical characteristics of groundnut shell particle reinforced polyactide nano fiber," *Revista Materia*, vol. 21, pp. 482-491, 2016.

[19] M. A. Usman, I. Momohjimoh, A. O. Usman, "Mechanical, physical and biodegradability performances of treated and untreated groundnut shell powder recycled polypropylene composites," *Material Research Express*, vol. 7, pp. 035302, 2020.

[20] C. Soni, P. K. Patnaik, S. K. Mishra, S. S. Panda, K. C. Rath, "Sisal fiber and groundnut shell particulate reinforced hybrid epoxy composites: A study on mechanical and tribological properties," *Materials Today Proceedings*, In Press, 2023.

[21] O. V. Potadar, G. S. Kadam, "Preparation and Testing of Composites Using Waste Groundnut Shells and Coir Fibers," *Procedia Manufacturing*, vol. 20, pp. 91-96, 2018.

[22] E. Garcia, J. F. Louvier-Hernandez, F. J. Cervantes-Vallejo, M. Flores-Martinez, R. Hernandez, L. A. Alcaraz-Caracheo, "Mechanical, dynamic and tribological characterization of HDPE/peanut shell composites," *Polymer Testing*, vol. 98, pp. 107075, 2021.

[23] D. D. C. V. Sheng, N. S. Ramegowda, V. Guna, N. Reddy, "Groundnut shell and coir reinforced hybrid bio composites as alternative to gypsum ceiling tiles," *Journal of Building Engineering*, vol. 57, pp. 104892, 2022.

[24] O. Oulidi, I. Elaaraj, M. Jabri, A. Nakkabi, A. Bouymajane, F. R. Filali, N. Fahim, E. Moualij, "Enhancing and hindering biodegradation: A comparative study on polyamide 6 reinforced with bio-fillers (peanut shell, olive pomace, and plaster)," *Sustainable Chemistry for the Environment*, vol. 7, pp. 100116, 2024.

[25] O. V. Potadar, G. S. Kadam, "Preparation and Testing of Composites Using Waste Groundnut Shells and Coir Fibers," *Procedia Manufacturing*, vol. 20, pp. 91-96, 2018.

[26] W. Baig, M. Mushtaq, "Investigation of mechanical properties and water absorption behaviour on tamarind shell fiber – Reinforced epoxy composite laminates," *Materials Today Proceedings*, vol. 45, pp. 440-446, 2020.

[27] S. Ramu, N. Senthilkumar, B. Deepanraj, "Experimental investigation on alkali treated (NaOH) groundnut shell (Arachis hypogaea L.) and rick husk (Oryza sativa) particle epoxy hybrid composites," *Materials Today Proceedings*, In Press 2023.

[28] R. Baptista, A. Mendao, M. Guedes, R. Marat-Mendes, "An experimental study on mechanical properties of epoxy-matrix composites containing graphite filler," *Procedia Structural Integrity*, vol. 1, pp. 74-81, 2016.

[29] M. A. G. Benega, W. M. Silva, M. C. Schnitzler, R. J. E. Andrade, H. Ribeiro, "Improvements in thermal and mechanical properties of composites based on epoxy-carbon nanomaterials – A brief landscape," *Polymer Testing*, vol. 98, pp. 107180, 2021.

[30] C. Y. Dang, K. Liu, M. X. Fan, S. Q. Zhu, S. H. Zhao, X. J. Shen, "Investigation on cryogenic interlaminar shear properties of carbon fabric/epoxy composites improved by graphene oxide-coated glass fibers," *Composites Communications*, vol. 22, pp. 100510, 2020.

[31] E. Sarikaya, H. Calloglu, H. Demirel, "Production of epoxy composites reinforced by different natural fibers and their mechanical properties," *Composites Part B: Engineering*, vol. 167, pp. 461-466, 2019.

[32] C. E. Shannon, "A Mathematical Theory of Communication," *The Bell System Technical Journal*, vol. 27, pp. 623–656, 1948.

[33] E. Wang, N. Alp, J. Shi, C. Wang, X. Zhang, H. Chen, "Multi-criteria building energy performance benchmarking through variable clustering based compromise TOPSIS with objective entropy weighting," Energy, vol. 125, pp. 197–210, 2017.

[34] R. Kumar, S. Singh, P. S. Bilga, Jatin., J. Singh, S. Singh, M. L. Scutaru, C. I. Pruncu, "Revealing the benefits of entropy weights method for multi-objective optimization in machining operations: A critical review," *Journal of Materials Research and Technology*, vol. 10, pp. 1471–1492, 2021.

[35] R. K. Thakur, K. K. Singh, "Impact of MWCNT in CFRP composite during end milling process," *Materials and Manufacuring Processes*, vol. 37, no. 7, pp. 816-824, 2021.

[36] S. Chakraborty, "TOPSIS and Modified TOPSIS: A comparative analysis," *Decision Analytics Journal*, vol. 2, pp. 100021.

[37] L. Lamrini, M. C. Abounaima, M. T. Alaoui, "New distributed-topsis approach for multi-criteria decision-making problems in a big data context," *Journal of Big Data*, vol. 10, pp. 97.